Artical ID:1006-3471(2010)03-0263-10

Comparative Study of Nanoporous Pt, PtRu and PtRuIr Catalysts Using Electrochemical FTIR Spectroscopy

Robert M. Amussen, Peter Holt-Hindle, Samantha Nigro, Aicheng Chen*
(*Department of Chemistry, Lakehead University, 955 Oliver Road, Thunder Bay, Ontario P7B 5E1, Canada*)

Abstract: In recent years much effort has been put towards developing efficient Pt-based electrocatalysts for applications in fuel cells. With the rising cost of precious metals such as Pt, the need to enhance the activity and to decrease the load of catalysts is prominent. Herein we report on the synthesis and comparative study of nanoporous Pt, PtRu and PtRuIr electrocatalysts. The nanoporous electrodes were fabricated using a hydrothermal method and characterized by scanning electron microscopy (SEM), energy dispersive spectroscopy (EDS), X-ray diffraction (XRD) and X-ray photoelectron spectroscopy (XPS). The electrocatalytic activity of the fabricated nanoporous materials was evaluated using both CO stripping experiments and methanol oxidation reactions, revealing that the addition of Ir greatly improved the activity of the nanoporous PtRu. To decipher the origin of the significant enhancement, in-situ electrochemical FTIR spectroscopy was employed to study the oxidation of methanol on the nanoporous Pt, PtRu and PtRuIr electrodes.

Key words: electrocatalysis; methanol oxidation; electrochemical FTIR; nanoporous PtRuIr
CLC Number: O646;O433.5 **Document Code:** A

1 Introduction

A worldwide increase in energy demands, coupled with increased pollution concerns and depleted fossil fuel reserves, has driven research toward novel means of creating energy with high efficiency and low emission[1]. Methanol and hydrogen powered fuel cells are potential solutions to this pressing problem, specifically direct methanol fuel cells (DMFCs) and proton exchange membrane fuel cells (PEMFCs)[2-4]. From the fuel consumption point of view, the DMFC is preferred over the PEMFC. Hydrogen still lacks a safe and reliable storage method; whereas methanol, with a higher energy density, is more easily stored and distributed at ambient temperatures. In the development of a practical catalyst, the high cost and inefficiency of Pt hinder its commercialization. CO_2 is the main product of methanol oxidation; however, other species such as CO, formaldehyde, formic acid and methyl formate also arise during the oxidation, creating possible multiple degradation mechanisms. The formation of CO is the most troublesome on Pt anodes, as CO can strongly adsorb to the catalytic sites, hindering the kinetics of methanol oxidation.

The Pt catalyst can be improved through advanced structural designs and the addition of a co-catalyst[5]. A wide variety of studies have been carried out to rectify this problem using various co-catalysts such as Ru[6], Sn[7], W[8], and Pb[9] coupled with Pt to enhance CO oxidation. An example of the enhancement of CO oxidation was shown by our group with a nanostructured PtRu electrocatalyst[10]. This catalyst showed high performance in the oxidation of both CO and methanol through the production of oxygen spe-

Received: 2010-06-26, Revised: 2010-07-09 * Corresponding author, Tel:(01-807)3438318; E-mail:achen@lakeheadu.ca
This work was supported by a Discovery Grant from the Natural Sciences and Engineering Research Council of Canada (NSERC).

cies. PtRu catalysts have become the research standard for comparison due to their strong performance[11]. On the other hand, our recent study has revealed that the addition of Ir significantly enhances the catalytic activity of Pt[12-13].

To determine the effect of the addition of Ir on the PtRu catalyst, nanoporous Pt, PtRu and PtRuIr electrocatalysts were synthesized and systemically investigated in this study. Our electrochemical study revealed that the incorporation of Ir greatly improved the activity of the nanoporous PtRu. Electrochemical Fourier transform infrared (FTIR) spectroscopy is a powerful technique used in the monitoring of reactions at the electrode interface[14-16]. To decipher the origin of the significant enhancement, *in-situ* electrochemical FTIR spectroscopy was employed to study the oxidation of methanol on the nanoporous Pt, PtRu and PtRuIr catalysts.

2 Experimental

2.1 Materials

Titanium plates (99.2%) from Alfa Aesar were used as the substrate. $H_2PtCl_6 \cdot 6H_2O$, $RuCl_3$, $IrCl_3$, methanol (99.9%), isopropyl alcohol (99.5%), formaldehyde (37% mass in water), hydrochloric acid (37.5%), and sulphuric acid (99.999%) from Aldrich were used as received. Nanopure® water (18.2 MΩ) was used to prepare all solutions.

2.2 Synthesis of Nanoporous Pt, PtRu and PtRuIr

A hydrothermal method was used to fabricate the nanoporous catalysts[17]. A Ti plate (1.25 cm × 0.8 cm × 0.05 cm) plate was washed via ultrasonication in acetone followed by Nanopure® water. The plates were then etched in an 18% HCl solution at 85 ℃ for 10 min. These plates were then placed in a Teflon® vessel along with a 10 mL solution containing the metal precursor, excess reducing agent and Nanopure® water. The precursors used were H_2PtCl_6 dissolved in Nanopure® water, and $RuCl_3$ and $IrCl_3$ dissolved in isopropanol. Formaldehyde was used as the reducing agent. The vessel was placed in the autoclave and heated at 180 ℃ for 10 h.

2.3 Instruments and Electrochemical Measurements

The surface morphology and composition of the Pt, PtRu and PtRuIr electrodes were characterized using scanning electron microscopy (SEM) (JEOL JSM 5900LV) equipped with an energy dispersive X-ray spectrometer (EDS) (Oxford Links ISIS). Surface elemental compositions based on quantitative EDS analysis are reported in average values of readings taken at five different spots on each sample surface. The X-ray diffraction (XRD) patterns of the as-prepared samples were recorded using a Philips PW 1050-3710 Diffractometer with Cu Kα radiation. XRD patterns were compared and assigned according to the database of the International Centre for Diffraction Data (ICDD). X-ray photoelectron spectra (XPS) (Omicron EA-125 energy analyzer and a multi-channel detector) were recorded using a monochromatic Mg Kα X-ray source ($h\nu = 1253.6$ eV). All binding energies (BE) reported here were corrected using the Cl $2p_{3/2}$ peak at 199 eV as an internal standard. Atomic sensitivity factors were employed for calculating the surface metallic compositions from the integrated peak areas.

Cyclic voltammetry (CV) and chronoamperometry (CA) were performed in a three-electrode system. A platinum coil served as the counter electrode and was annealed prior to each experiment. The reference electrode was a saturated calomel electrode (SCE) connected through a salt bridge. Data acquisition for the CV and CA experiments was performed on a VoltaLab 40. For the CO-stripping experiments, the potential was held constant at −0.1 V for 740 s. CO (PRAXAIR, 99.9%) was bubbled through the solution for 600 s; the solution was then de-aerated with ultra-pure argon (99.999%) for 120 s; finally the solution was left to rest for 20 s. Argon was passed over the top of the electrolyte solution during the experiments.

The electrochemical FTIR experiments were performed on a Thermo Nicolet 8700 equipped with a MCT-B detector cooled with liquid N_2. The electrochemical cell was a Teflon cylinder, specially designed

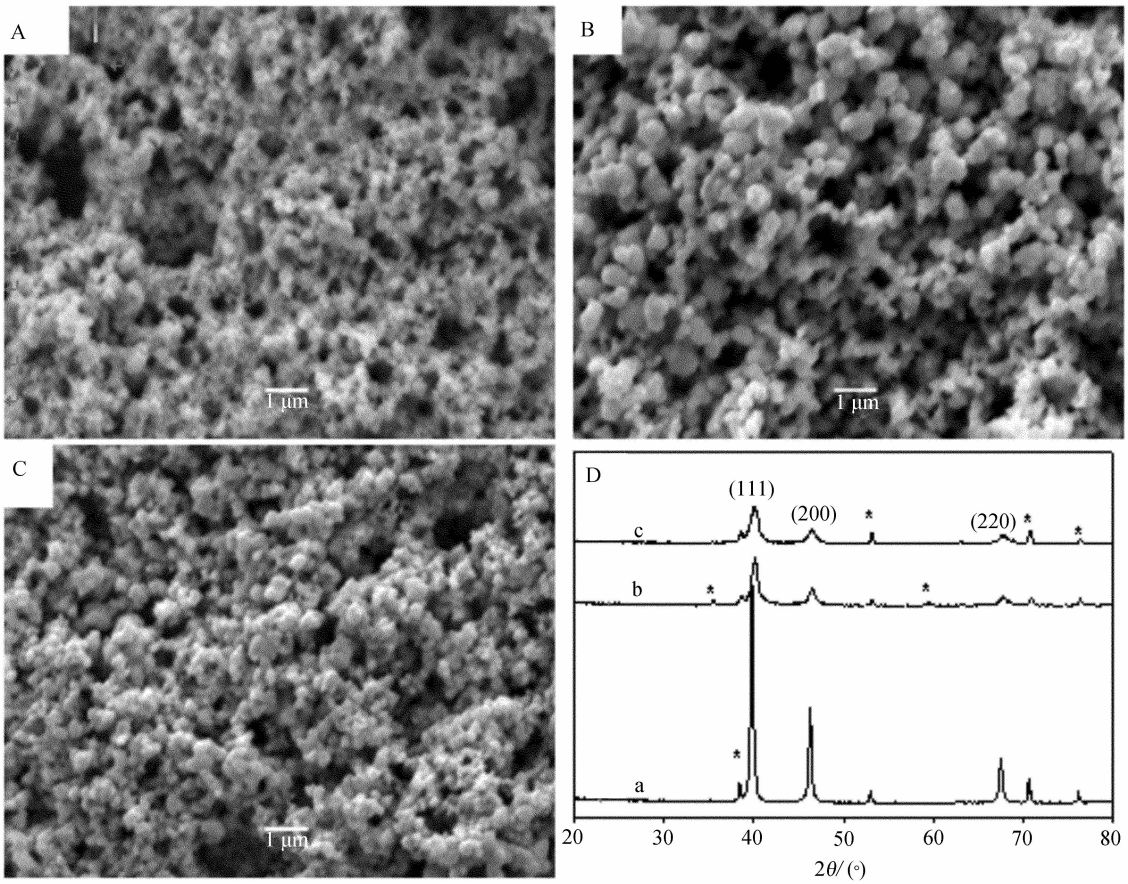

Fig. 1　SEM images of nanoporous Pt (A), PtRu (B), PtRuIr (C), and their corresponding XRD patterns (D)
* indicates the peaks derived from Ti substrate

to hold the internal reflection element (IRE) above the ATR mirrors, and completely sealed from the external environment. The IRE used in this study was a semi-hemispherical ZnSe crystal. Prior to each experiment, the ZnSe window was polished with alumina powder. Two configurations were used in our FTIR studies. For the first configuration used to monitor the species formed on the electrocatalysts, the Pt, PtRu and PtRuIr nanomaterials synthesized from the hydrothermal technique were transferred to water, where they became a suspension upon ultrasonication. The suspension was placed onto the ZnSe crystal surface to form a thin layer. In this arrangement, species which desorb from the electrode surface are lost to the bulk solution, thus becoming undetectable in the FTIR spectra. To overcome this problem, a second setup to monitor these desorbed species was employed. A Ti disk electrode with a diameter of 1.5 cm was pressed to the surface of the IR window, trapping a thin layer of solution. The thin layer of electrolyte was renewed every time before the potential E_2 was changed. The Ti disks were etched in an 18% HCl solution at 85 ℃ for 10 min first; and then nanoporous Pt, PtRu and PtRuIr coatings were directly grown on the treated Ti disks with the hydrothermal technique described previously. A Pt-coil was used as the counter electrode, and SCE served as a reference for all the electrochemical FTIR experiments. Upon adding a 0.1 mol · L^{-1} CH_3OH + 0.5 mol · L^{-1} H_2SO_4 solution to the FTIR cell, the solution was purged with ultra high purity argon. A base spectrum, $R(E1)$, was collected at −200 mV. The potential was then stepped up in 100 mV increments while the $R(E2)$ spectrum was recorded. The number of scans for each spectrum is 400. The final spectrum was calculated using the following equation[15,18]:

$$\Delta R/R = [R(E2) - R(E1)]/R(E1)$$

All experiments were carried out at ambient tem-

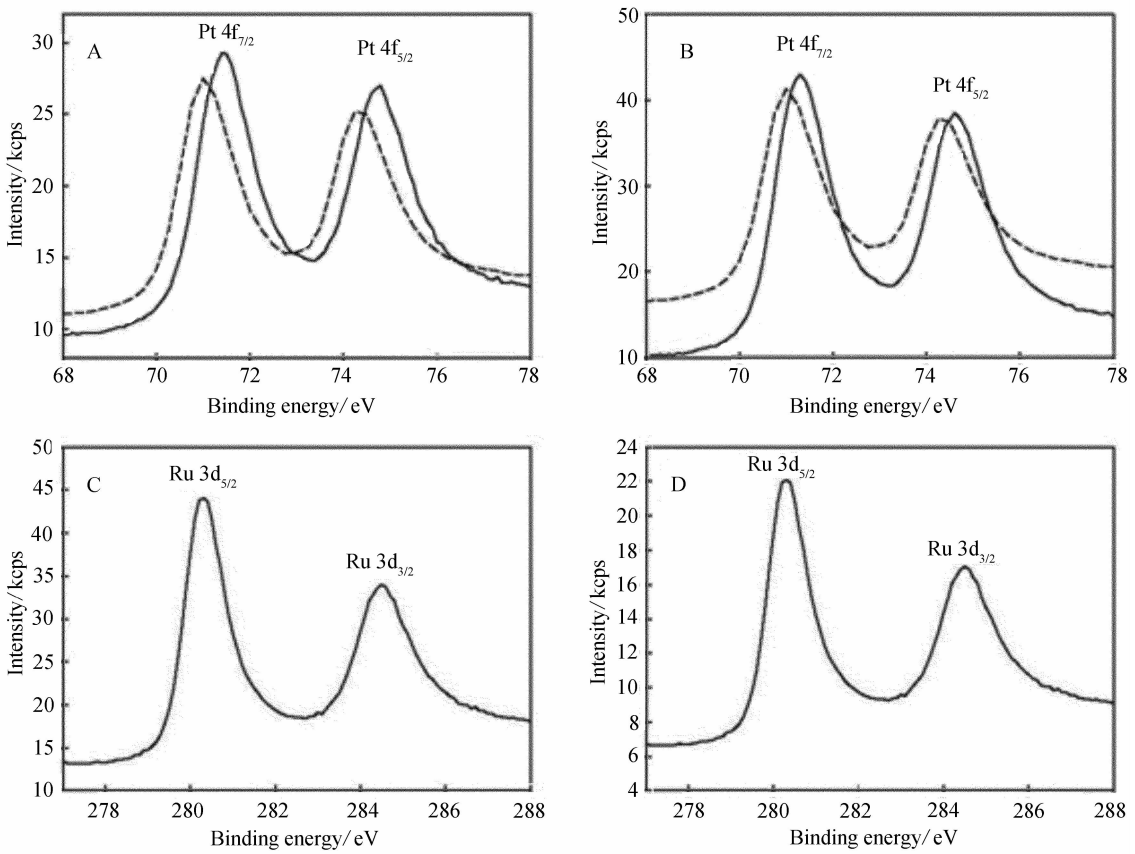

Fig. 2 XP spectra of the Pt 4f region of PtRu (A) and PtRuIr (B), Ru 3d region of PtRu (C) and PtRuIr (D) nanoporous Pt (dashed line) is included for comparison

perature (20 ± 2 ℃).

3 Results and Discussion

3.1 Surface Characterization

The surface morphology of the nanoporous-Pt networks was studied using SEM at 10000 × magnification. Fig. 1 shows the electrode surfaces of (A) nanoporous Pt(A), PtRu (B), PtRuIr (C), all of which display high surface coverage of the Ti substrate with random distribution of pores throughout the catalyst network. The PtRu and PtRuIr samples show particle sizes ranging from 50 ~ 500 nm with pores ranging from tens of nanometers to several micrometers in diameter. EDS analysis was performed on the samples to determine their composition. From the quantitative study it was found that the composition of the samples is: pure Pt (A); PtRu with 40% Ru (B); and PtRuIr with 30% Ru and 15% Ir (C), confirming the expected results from the composition of the precursor solutions.

XRD analysis was used to characterize the phase and structure of the as-synthesized nanoporous electrodes. As shown in Fig. 1D, the nanoporous Pt (a), PtRu (b) and PtRuIr (c) electrodes all display the (111), (200) and (220) reflections characteristic of a face centered cubic (*fcc*) crystal structure. In comparison to nanoporous Pt, the PtRu and PtRuIr peaks have a positive shift in the 2θ values, which corresponds to decreased *d*-spacing values and lattice constants. Further quantitative calculation on the lattice constant a of the diffraction angles of the (220) reflection peak revealed the a values of 0.392, 0.390 and 0.390 nm for nanoporous Pt, PtRu and PtRuIr, respectively. All the above results indicate that the formation of PtRu and PtRuIr alloys[17,19-21].

The presence of metallic interactions between the components was studied with XPS. In Fig. 2A, two 4f binding peaks of Pt, identified as $4f_{7/2}$ and $4f_{5/2}$, are evident for the nanoporous Pt (dashed line) and PtRu electrodes (solid line). The Pt $4f_{7/2}$ and $4f_{5/2}$ doublets of

the nanoporous Pt occur at 71.0 and 74.3 eV and at 71.3 and 74.7 eV for the nanoporous PtRu electrode. In Fig. 2B, the Pt $4f_{7/2}$ and $4f_{5/2}$ doublets of the nanoporous PtRuIr electrode (solid line) occur at 71.4 and 74.8 eV. The Ir $4f_{7/2}$ and $4f_{5/2}$ doublets for the PtRuIr electrode (data not shown) occur at 60.6 and 63.6 eV versus the values for Ir metal of 60.9 and 63.9 eV[22]. Fig. 2C and 2D show that the Ru $3d_{5/2}$ and $3d_{3/2}$ binding peaks occur at 280.2 and 284.4 eV for the PtRu electrode (2C) and at 280.3 and 284.5 eV for the PtRuIr electrode (2D), compared to 280.0 and 284.0 eV for pure Ru metal[23]. Since a shift in the binding energy of core-level orbitals corresponds with a change in electron density, this indicates the presence of an electronic interaction between Pt and Ru and/or Ir.

3.2 CO Oxidation on PtRuIr Electrodes

CO has been identified as both an intermediate and poisoning species in the oxidation pathways of formic acid[24], methanol[25], and other small organic molecules on Pt. A desired characteristic of potential catalysts is a penchant towards removal of surface CO. At low potentials, CO can adsorb strongly to the Pt catalyst surface, thus inhibiting its performance. CO oxidation experiments, as described in 2.3, on the three nanoporous networks were performed in 0.5 mol · L^{-1} H_2SO_4 and the results are presented in Fig. 3.

The flat line at the beginning of the forward sweep in the hydrogen adsorption region shows that hydrogen adsorption to the catalyst surface is completely repressed due to the adsorption of CO to the surface. In the region from 0 to 600 mV a small, broad shoulder wave followed by a sharp peak representing CO oxidation can be seen for all three electrodes. In the reverse scan, the distinctive hydrogen adsorption/desorption peaks return and the CV resembles that of a CO free environment in H_2SO_4, showing complete removal of the adsorbed CO.

Nanoporous Pt shows an onset potential of 138 mV for the oxidation of adsorbed CO, while reaching its peak at 468 mV. Slightly out-performing this is the PtRu with an onset of CO oxidation at 15 mV and peak potential of 444 mV. This is due to the Ru sites

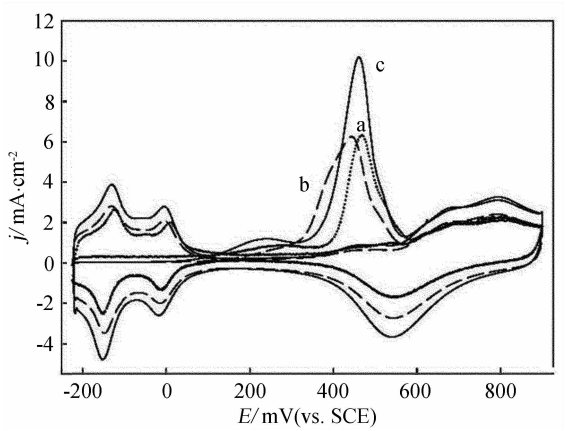

Fig. 3　The oxidation of CO at a scan rate of 20 mV/S in 0.5 mol · L^{-1} H_2SO_4 on the nanoporous Pt (dotted) (a), PtRu (dashed) (b), and PtRuIr (solid line) electrodes (c)

on the nanoporous network generating oxygen species which serve to oxidize the adsorbed CO. The PtRuIr trimetallic electrode shows the greatest performance, with an onset potential of −47 mV and the highest current density at a peak potential of 450 mV. It is believed that this improvement can be attributed to the presence of Ir assisting in producing and stabilizing additional oxygen species, which in turn oxidize the adsorbed CO on the Pt sites.

The stripping of CO can also be used as a means of calculating the electroactive surface area of the catalysts[26-27]. The consumed charges for the hydrogen adsorption/desorption from the CO stripping, calculated through the area under the CO oxidation peak are 19.98 mC, 25.98 mC and 30.32 mC for nanoporous Pt (a), PtRu (b), and PtRuIr, respectively (c). By assuming a charge to surface area value of 420 μC/cm^2 for this process[18], the electroactive surface areas (ESA) of the electrodes were found to be 47.6, 67.9, 72.2 cm^2 for nanoporous Pt (a), PtRu (b), and PtRuIr (c), respectively, which are much higher than their geometric surface area (1 cm^2).

3.3 Electrochemical Oxidation of Methanol

The electrochemical oxidation of methanol on the nanoporous Pt, PtRu and PtRuIr electrodes was investigated using cyclic voltammetry with a 0.1 mol · L^{-1} CH_3OH + 0.5 mol · L^{-1} H_2SO_4 solution and at a scan

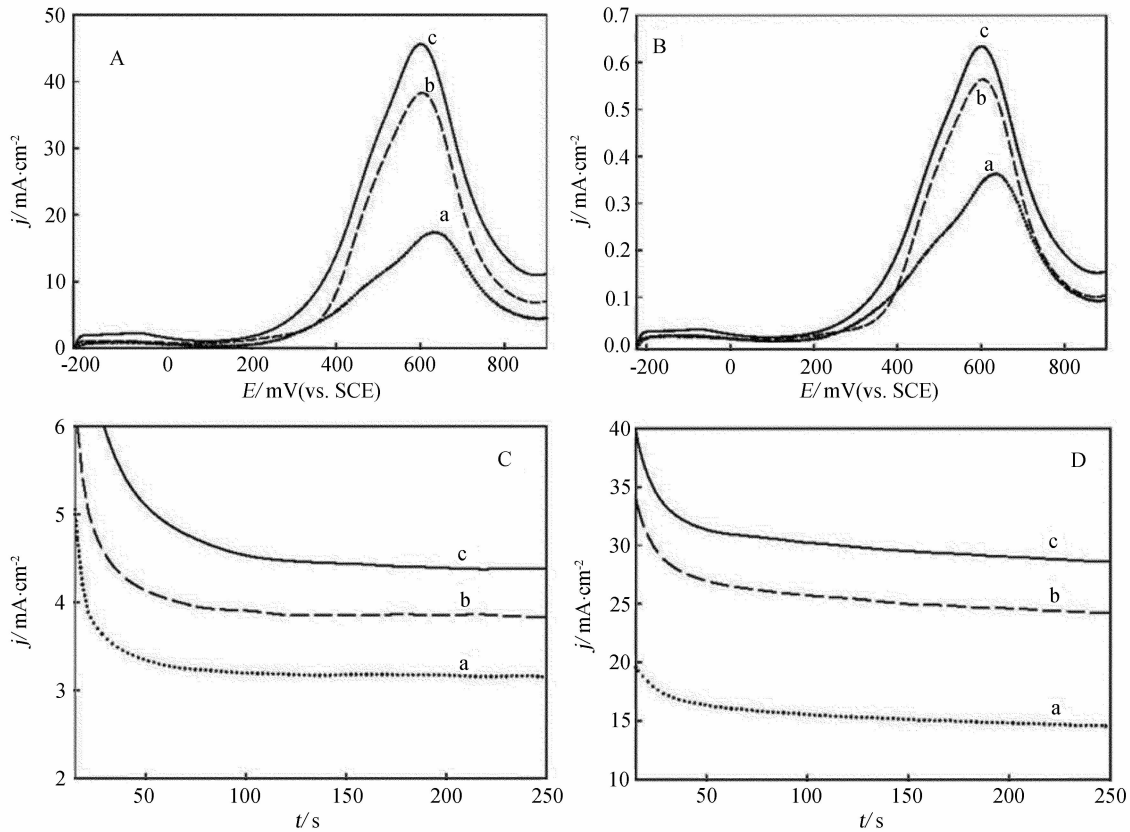

Fig. 4 Cyclic voltammogram recorded in 0.1 mol · L^{-1} CH_3OH + 0.5 mol · L^{-1} H_2SO_4 (A); the corresponding cyclic voltammograms calculated based on the electroactive surface area (B), chronoamperometric curves measured in 0.5 mol · L^{-1} H_2SO_4 + 0.1 mol · L^{-1} CH_3OH at potentials of +300 mV (C) and +600 mV (D) a. nanoporous Pt; b. PtRu; c. PtRuIr

rate of 20 mV/s. The resulting voltammograms are displayed in Fig. 4A. For the sake of clarity, only the forward scans are shown. Comparison of curve a and b shows that the addition of Ru to Pt significantly increases the peak current density of the oxidation of methanol. The oxidation of methanol with the trimetallic PtRuIr (Curve c) shows further improvement through the addition of Ir to the PtRu catalyst, producing a peak current density of 46 mA/cm^2. The addition of Ir also lowers the onset potential of methanol oxidation.

As seen in Section 3.2, the nanoporous PtRuIr electrode possesses the highest ESA. Now the question is whether the significant increase of the current for methanol oxidation on the trimetallic electrode is simply due to the increase of the ESA. To answer this question, Fig. 4B presents the methanol oxidation curves with the current densities corrected for the electroactive surface area instead of the geometric surface area. As seen in Fig. 4B, the nanoporous PtRu outperforms the nnaoporous Pt; The PtRuIr shows the highest activity towards the methanol oxidation. The performance enhancement of the trimetallic alloy is also evident in a study of the steady state current densities of the electrodes. The potential was held at 0 mV for 60 s prior to stepping the potential up to 300 mV or 600 mV where the potential was held for 500 s. 300 mV is approximately the onset potential for methanol oxidation for all three electrodes, while 600 mV is close to the peak potential as seen in Fig. 4A, Fig. 4C and 4D display the amperometric responses of the Pt (a), PtRu (b) and PtRuIr (c) at 300 and 600 mV, respectively. After 200 s all the electrodes achieve their steady-state currents. The same trend is observed at both electrode potentials 300 and 600 mV; the PtRuIr achieves the highest steady state current compared to the Pt and PtRu electrode. To decipher the origin of the enhancement, we further studied the electrochemical oxidation of methanol on these three kinds of electrodes using electrochemical FTIR spec-

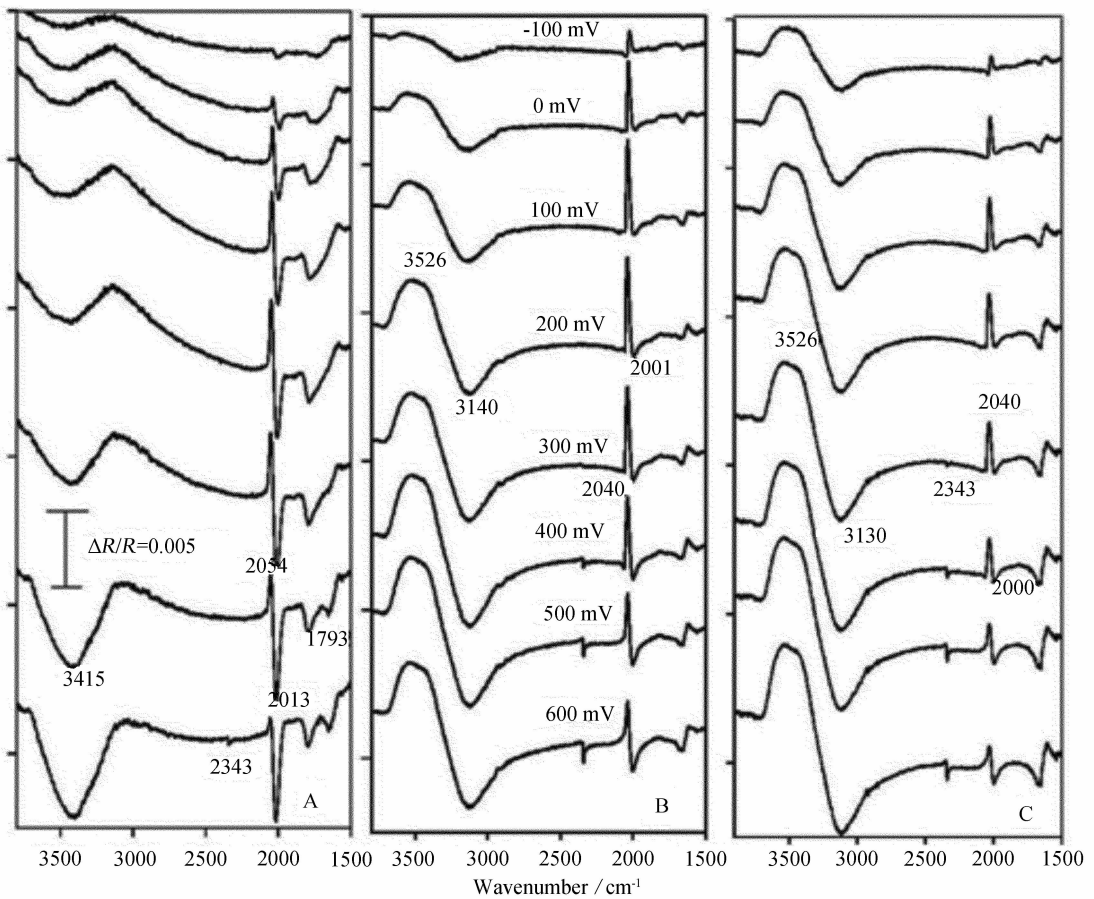

Fig. 5　Electrochemical FTIR spectra for nanoporous Pt (A), PtRu (B), and PtRuIr recorded in 0.1 mol · L^{-1} CH_3OH + 0.5 mol · L^{-1} H_2SO_4 (C)　scans: 400; resolution: 4 cm^{-1}; $E1$ = −200 mV

troscopy.

3.4 Electrochemical FTIR Studies

Fig. 5 presents the electrochemical FTIR spectra recorded in 0.1 mol · L^{-1} CH_3OH + 0.5 mol · L^{-1} H_2SO_4, where the base potential ($E1$) was fixed at −200 mV and the sample potential ($E2$) was varied from −100 to 600 mV. As seen in Fig. 5A, the intensity of the broad negative going peak centered at 3415 cm^{-1} increases with the increment of $E2$, which can be attributed to the formation of OH species on the nanoporous Pt surface[3]. Due to the design of our IR system, CO_2 is free to exit the electrode surface to the bulk solution; however, at the high potential ($E2$ = 600 mV), a peak at 2343 cm^{-1} is observed, confirming the formation of CO_2 from the complete oxidation of methanol. An abnormal bipolar band with a positive-going peak centered at around 2054 cm^{-1} and a negative-going peak at 2013 cm^{-1} from linearly bonded CO (CO_L) is also observed. This abnormal phenomenon has been reported by Sun and co-workers[28]. The appearance of the negative-going peak at 1803 cm^{-1} reveals the formation of bridged CO (CO_B) on the surface.

Fig. 5B displays the spectra collected on the PtRu electrocatalyst. Instead of the negative-going peak at 3415 cm^{-1} on the Pt surface (Fig. 5A), a large bipolar band is observed on the PtRu surface, having the positive peak at 3526 cm^{-1} and the negative portion centered at 3140 cm^{-1}. Obviously, this bipolar feature arises due to the presence of Ru. This is due to OH species being formed at the Ru sites at lower potentials than Pt and the ν(OH) of Ru-OH appearing at a higher frequency than that of Pt-OH[3]. The CO_2 peak centered at 2343 cm^{-1} (CO_2) appears at 400 mV, which is 200 mV lower compared to Fig. 5A. Although the bipolar CO_L peak is observed, no CO_B

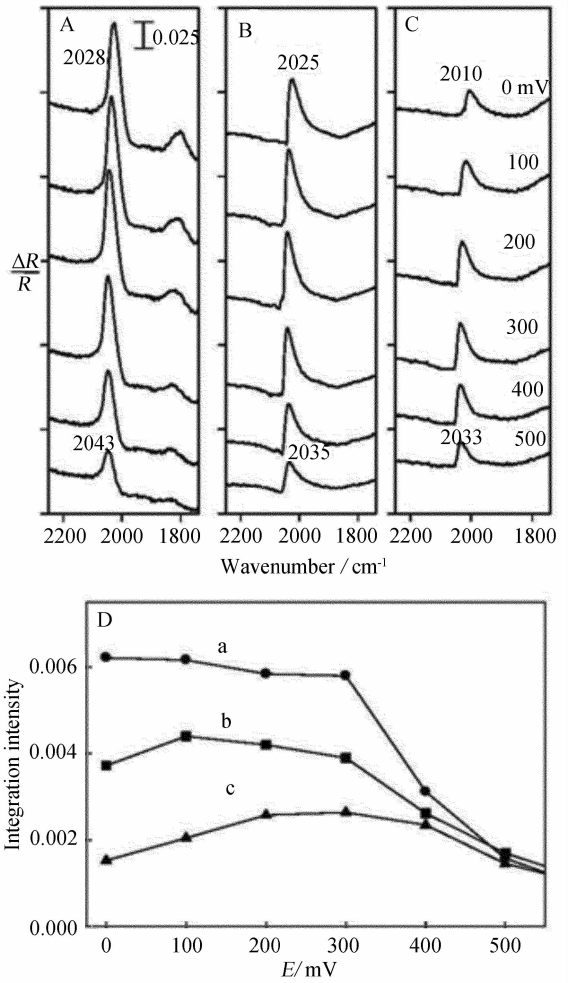

Fig. 6 Electrochemical FTIR spectra shown in the CO region for nanoporous Pt (A), PtRu (B), PtRuIr with $E1 = 1000$ mV (C), and the corresponding integrated intensity of total CO bands (D)

peak appears in Fig. 5B. Fig. 5C presents the electrochemical FTIR spectra of methanol oxidation on the PtRuIr surface, showing similar features to the PtRu electrode (Fig. 5B). Interestingly, the bipolar band in the ν(OH) region appears at a lower potential and with higher intensity. In addition, the CO_2 peak at 2343 cm^{-1} appears at a lower potential (300 mV). All these results show that the incorporation of Ir further enhances the catalytic activity of PtRu.

As seen in Fig. 5, it is difficult to quantitatively compare the amount of CO formation due to the bi-polar feature. To quantitatively determine the CO formation on these electrodes during the methanol oxidation, we recorded a base spectrum at $E1 = 1000$ mV, where the catalyst surface is free of CO. The resulting FTIR spectra with the spectrum collected at $E1 =$ 1000 mV as the reference are displayed in Fig. 6. Two positive-going peaks appear at 2027 and 1803 cm^{-1} (Fig. 6A), corresponding to the CO_L and CO_B IR absorption. Only the CO_L peak is seen for both the PtRu (Fig. 6B) and PtRuIr (Fig. 6C) electrodes. As expected, a shift of the CO_L band is observed as the $E2$ is increased due to the Stark effect[15-16]. For the nanoporous Pt surface (Fig. 6A), the CO_L band appears at 2028 cm^{-1} at $E2 = 0$ mV, and shifts to 2043 cm^{-1} when the $E2$ was increased to 600 mV. The CO_L band shifts from 2025 to 2035 cm^{-1} for the nanoporous PtRu electrode and from 2010 to 2033 cm^{-1} for the PtRuIr electrode when the $E2$ was increased from 0 to 600 mV. Fig. 6D presents the total integration intensity of the CO peaks, showing that the formed CO on the surface decreases in the following order: Pt > PtRu > PtRuIr.

CO_2, as the final product of methanol oxidation, provides an accurate account of the efficiency of the catalyst. To quantitatively compare the production of CO_2 resulting from the electrochemical oxidation of methanol, the second IR configuration was employed as described in the experimental section. The species desorbed from the electrode surface may appear in the IR spectrum as they are trapped in the thin layer between the electrode surface and the IR window. The main feature to be investigated here is the appearance and intensity of the CO_2 band centered at 2343 cm^{-1}. As shown in Fig. 7, the onset potential of CO_2 formation is decreased from 300 mV (7A) to 200 mV (7B) and to 100 mV (7C), revealing that the PtRuIr has the lowest onset potential for methanol oxidation. Fig. 7D presents the integration intensity of the CO_2 peak. As can be seen, the largest amount of CO_2, and thus the largest extent of methanol oxidation through higher performance, comes from the PtRuIr electrode. All these IR results are consistent with the cyclic voltammetric and chronoamperometric studies.

4 Conclusions

In summary, we have fabricated and systematically studied nanoporous Pt, PtRu and PtRuIr catalysts. Our CO-stripping experiments reveal that the formed nanoporous structures possess a very high electroactive surface area and that the addition of Ru

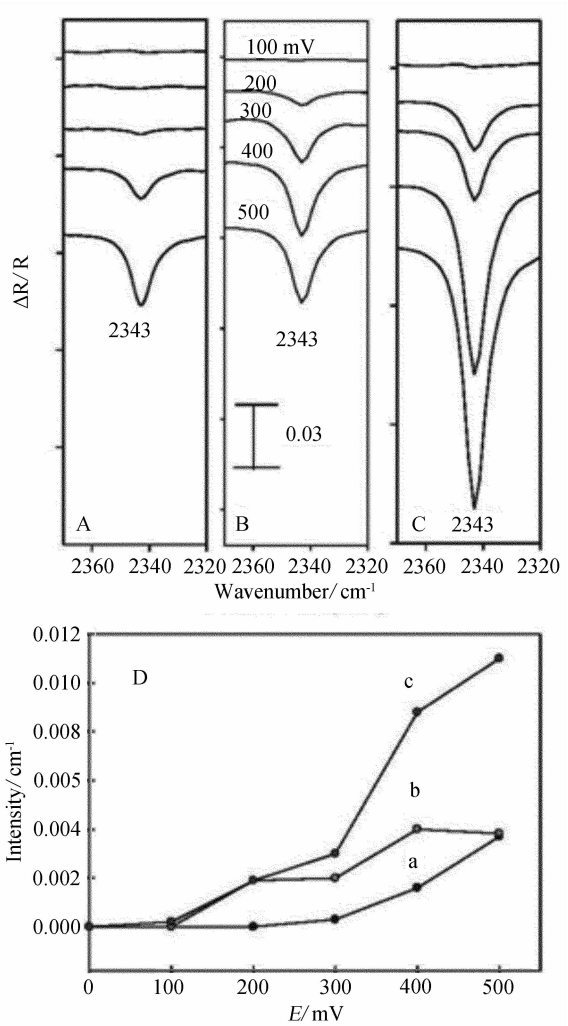

Fig. 7　Electrochemical FTIR spectra shown in the CO_2 region recorded in 0.1 mol · L^{-1} CH_3OH + 0.5 mol · L^{-1} H_2SO_4 for Pt (A), PtRu (B), and PtRuIr with the second IR configuration (C); and the corresponding integrated intensity of the CO_2 peak (D)

and RuIr lowers the onset potential of CO oxidation. The cyclic voltammotric and chronoamperometric studies show that the incorporation of Ru significantly improves the Pt activity towards methanol oxidation and that the addition of Ir further enhances the performance of PtRu. The XRD and XPS studies show that alloyed PtRu and PtRuIr were formed and that there are electronic interactions among the metals. Our electrochemical FTIR studies provide insights on why the presence of Ru and RuIr improves the activity of the Pt-based catalyst. The bipolar feature of the υ_{OH} band observed with the PtRu and PtRuIr electrodes show the incorporation of Ru and RuIr facilitates the formation of OH-like species which aids the oxidation of the poisoning CO intermediate. The quantitative analysis of the CO and CO_2 bands reveals that the presence of Ru and RuIr significantly lower the formation of CO on the surface, leading to a large increase of the CO_2 production.

References:

[1] Liu H, Zhang L, Zhang J, et al. A review of anode catalysis in the direct methanol fuel cell [J]. J of Power Sources, 2006, 155: 95-110.

[2] Chen A, Holt-Hindle P. Platinum-based nanostructured materials: Synthesis, properties and applications [J]. Chem Rev, 2010, 110: 3767-3804.

[3] Yajima T, Uchida H, Watanabe M. In-situ ATR-FTIR spectroscopic study of electro-oxidation of methanol and adsorbed CO at Pt-Ru alloy[J]. J Phys Chem B, 2004, 108: 2654-2659.

[4] Tian N, Zhou Z Y, Sun S G, et al. Synthesis of tetrahexahedral platinum nanocrystals with high-index facets and figh electro-oxidation activity [J]. Science, 2007, 316: 732-735.

[5] Xia M, Wang Q, Eikerling M, et al. Effectiveness factor of Pt utilization in cathode catalyst layer of polymer electrolyte fuel cells [J]. Can J Chem, 2008, 86: 657-667.

[6] Peng X, Koczkur K, Chen A. Synthesis and characterization of ruthenium decorated nanoporous platinum materials[J]. Nanotechnology, 2007, 18: 305605.

[7] Jiang L H, Sun G Q, Sun S G, et al. Structure and chemical composition of supported Pt-Sn electrocatalysts for ethanol oxidation[J]. Electrochim Acta, 2005, 50, 5384-5389.

[8] Jayaraman S, Jaramillo T F, Baeck S H, et al. Synthesis and characterization of Pt-WO_3 as methanol oxidation catalysts for fuel cells[J]. J Phys Chem B, 2005, 109: 22958-22966.

[9] Raychowdhury C, Matsumoto F, Zeldovich V B, et al. Synthesis, characterization, and electrocatalytic activity of PtBi and PtPb nanoparticles prepared by borohydride reduction in methanol[J]. Chem Mater, 2006, 18: 3365-3372.

[10] Koczkur K, Yi Q, Chen A. Nanoporous Pt-Ru networks and their electrocatalytical properties[J]. Adv Mater, 2007, 19: 2648-2652.

[11] Basnayake R, Li Z, Lakshmi S, et al. PtRu nanoparticle electrocatalyst with bulk alloy properties prepared through a sonochemical method [J]. Lang, 2006, 22: 10446-10450.

[12] Holt-Hindle P, Yi Q, Wu G, et al. Electrocatalytic ac-

tivity of nanoporous Pt-Ir materials towards methanol oxidation and oxygen reduction[J]. J Electrochem Soc, 2008,155,K5-K9.

[13] Holt-Hindle P, Nigro S, Asmussen R M, et al. Amperometric glucose sensor based on Pt-Ir nanomaterials [J]. Electrochem Commun, 2008, 10: 1438-1441.

[14] Yan Y G, Li Q X, Huro S J, et al. Ubiquitous strategy for probing ATR surface – enhanced infrared absorption at platinum group metal-electrolyte interfaces [J]. J Phys Chem B, 2005, 109: 7900-7906.

[15] Sun S G, Chen A C. in-situ FTIRS Features during oxygen-adsorption and carbon-monoxide oxidation at a platinum electrode in dilute alkaline solutions [J]. J Electroanal Chem, 1992, 323: 319-328.

[16] Sun S G, Christensen P A, Wieckowski A. In-situ spectroscopic studies of adsorption at the electrode and electrocatalysis, Elsevier, Netherlands 2007.

[17] Wang J, Holt-Hindle P, MacDonald D, et al. Synthesis and electrochemical study of Pt-based nanoporous materials[J]. Electrochim Acta, 2008, 53: 6944-6951.

[18] Chen A, Lipkowski J. Electrochemical and spectroscopic studies of hydroxide adsorption at the Au(111) electrode[J]. J Phys Chem B, 1999, 103: 682-691.

[19] Ioroi T, Yasuda K. Platinum-iridium alloys as oxygen reduction electrocatalysts for polymer electrolyte fuel cells[J]. J Electrochem Soc, 2005, 152: A1917-1924.

[20] Gasteiger H A, Markovic N, Ross Jr P N, et al. Methanol electrooxidation on well characterized Pt-Ru alloys [J]. J Phys Chem, 1993, 97: 12020-12029.

[21] Arico A S, Antonucci P L, Modica E, et al. Effect of Pt-Ru alloy composition on high-temperature methanol electro-oxidation[J]. Electrochim Acta, 2002, 47: 3723-3732.

[22] Wagner C D, Riggs W M, Davis L E, et al. Handboook X-ray photoelectron spectroscopy [M]. Perkin-Elmer Co, 1979.

[23] Aric A S, Creti P, Kim H, et al. Analysis of the electrochemical characteristics of a direct methanol fuel cell based on a Pt-Ru/C anode catalyst[J]. J Electrochem Soc, 1996, 143: 3950-3959.

[24] Chen Y A, Ye S, Heinen M, et al. Application of in-situ attenuated total reflection-Fourier transform infrared spectroscopy for the understanding of complex reaction mechanism and kinetics: Formic acid oxidation on a Pt film electrode at elevated temperatures [J]. J Phys Chem B, 2006, 110: 9534-9544.

[25] Casado-Rivera E, Volpe D J, Alden L, et al. Electrocatalytic activity of ordered intermetallic phases for fuel cell applications[J]. J Am Chem Soc, 2004, 126: 4043-4049.

[26] Yeager E, Bockris J O, Conway B E, et al. Comprehensive treatise of electrochemistry, Electrodics: Experimental Techniques [M]. Vol. 9, Plenum Press, New York, 1984.

[27] Wang J, Adams B, Asmussen R M, et al. Facile synthesis and electrochemical Properties of Intermetallic PtPb Nanodendrites[J]. Chem Mater, 2009, 21: 1716-1724.

[28] Lu G Q, Sun S G, Cai LR, et al. In situ FTIR spectroscopic studies of adsorption of CO, SCN^-, and poly(o-phenylenediamine) on electrodes of nanometer thin films of Pt, Pd, and Rh: Abnormal infrared effects (AIREs)[J]. Lang, 2000, 16: 778-786.

纳米多孔 Pt,PtRu 及 PtRuIr 催化剂的电化学 FTIR 光谱之比较

Robert M. Amussen, Peter Holt-Hindle, Samantha Nigro, Aicheng Chen*

(加拿大湖首大学化学系,加拿大 安大略)

摘要: 近年来,致力于 Pt 基电催化剂在燃料电池中的应用已取得显著成果. 但随贵金属(如 Pt)成本的增加,提高催化剂的活性以及降低负载量的需求也日益迫切. 为此,作者合成并比较了纳米多孔 Pt, PtRu 及 PtRuIr 3 种电催化剂. 以扫描电镜(SEM)、能量色散谱(EDS)、X 射线衍射(XRD)和 X 射线光电子能谱(XPS)表征水热法制得的纳米多孔电极. CO 汽提实验和甲醇氧化反应测试上述纳米多孔材料的电催化活性. 结果表明,添加 Ir 极大改善纳米多孔 PtRu 的活性. 采用现场电化学 FTIR 光谱技术研究纳米多孔 Pt, PtRu 及 PtRuIr 电极上的甲醇氧化反应,以进一步揭示这种显著增强效应的成因.

关键词: 电催化作用; 甲醇氧化; 电化学 FTIR; 纳米多孔 PtRuIr